Soft-gluon corrections for single top quark production in association with electroweak bosons

Matthew Forslund* and Nikolaos Kidonakis

*Department of Physics, Kennesaw State University,
Kennesaw, GA 30144, USA*

Abstract: We present results for higher-order soft-gluon radiative corrections for single top-quark production in association with electroweak bosons, including $t\gamma$ and tZ production via anomalous FCNC couplings. We provide results for the total cross sections and differential distributions at LHC energies. We use K-factors to show the significance of the corrections compared to leading order, and we discuss uncertainties and the importance of the results.

1   Introduction

Top-quark production at the Large Hadron Collider (LHC) remains an active area of searches for physics beyond the Standard Model, including searches for anomalous couplings [1–3]. In some new physics models, top quarks can be produced via processes involving flavor-changing neutral currents (FCNC). Two such processes are the production of $t\gamma$ [4–11] and tZ [4,5,8–10,12,13] pairs without additional quarks in the final state.

The effective Lagrangian involving anomalous FCNC couplings of a tq pair to electroweak bosons, with q an up or charm quark, is given by

$$\Delta\mathcal{L}^{eff} = \frac{1}{\Lambda}\,\kappa_{tqA}\,e\,\overline{t}\,\sigma_{\mu\nu}\,q\,F_A^{\mu\nu} + h.c., \tag{1}$$

where κ_{tqA} is the anomalous coupling, with A a photon or Z-boson, Λ is an effective scale which is taken to be the top-quark mass, $F_A^{\mu\nu}$ are the appropriate electroweak-boson field tensors, and $\sigma_{\mu\nu} = (i/2)(\gamma_\mu\gamma_\nu - \gamma_\nu\gamma_\mu)$ where γ_μ are the Dirac matrices.

To improve experimental limits on these anomalous FCNC couplings, it is important to have a good theoretical prediction, which entails studying higher-order corrections. We calculate higher-order corrections to $gq \to tZ$ and $gq \to t\gamma$ arising from soft-gluon radiation. These soft-gluon corrections enhance the leading-order (LO) cross sections, and they dominate (and thus approximate well) the higher-order corrections. The approximate next-to-leading order (aNLO) and approximate next-to-next-to-leading order (aNNLO) corrections from soft-gluon emission were studied for the processes $gq \to tZ$ and $gq \to t\gamma$ in [14] and [15], respectively. We present detailed results for cross sections and differential distributions for both processes at LHC energies through aNNLO, and also some approximate next-to-next-to-next-to-leading order (aNNNLO) results. More details on soft-gluon resummation and top-quark production can be found in the review in Ref. [16].

2   Soft-gluon corrections

For the partonic process $g(p_g) + q(p_q) \to t(p_t) + A(p_A)$, where A represents a Z-boson or a photon, we define the kinematical variables $s = (p_g + p_q)^2$, $t = (p_g - p_t)^2$, $u = (p_q - p_t)^2$, and $s_4 =$

$s + t + u - m_t^2 - m_A^2$, where $m_A = m_Z$ for the Z-boson mass and $m_A = m_\gamma = 0$ for the photon, and m_t is the top-quark mass. Near partonic threshold, i.e. when there is just enough energy to produce the final tA state, but with the top quark and electroweak boson not necessarily at rest, we have $s_4 \to 0$. We also define $t_1 = t - m_t^2$, $t_2 = t - m_A^2$, $u_1 = u - m_t^2$, and $u_2 = u - m_A^2$.

We consider the double-differential partonic cross section $d^2\hat{\sigma}_{gq \to tA}^{(n)}/(dt\,du)$ at nth order. The LO cross section is

$$\frac{d^2\hat{\sigma}_{gq \to tA}^{(0)}}{dt\,du} = F_{gq \to tA}^{\text{LO}}\,\delta(s_4)\,, \tag{2}$$

where

$$
\begin{aligned}
F_{gq \to tA}^{\text{LO}} &= \frac{e^2 \alpha_s \kappa_{tqA}^2}{6 s^3 t_1^2}\left\{2m_t^6 - m_t^4(3m_A^2 + 4s + 2t) + m_t^2\left[2m_A^4 - m_A^2(2s+t) + 2(s^2 + 4st + t^2)\right]\right. \\
&\quad + 2m_A^6 - 4m_A^4 t + m_A^2(s+t)(s+5t) - 2t(3s^2 + 6st + t^2) \\
&\quad \left. - \frac{t}{m_t^2}\left[2m_A^6 - 2m_A^4(s+t) + m_A^2(s+t)^2 - 4st(s+t)\right]\right\}\,, \tag{3}
\end{aligned}
$$

with α_s the strong coupling.

The structure of the soft-gluon corrections is governed by a soft anomalous dimension, Γ^S. For next-to-leading-logarithm (NLL) accuracy, we need one-loop results. The one-loop expression for the soft anomalous dimension in Feynman gauge is given by

$$\Gamma_{gq \to tA}^{S\,(1)} = C_F\left[\ln\left(\frac{-u_1}{m\sqrt{s}}\right) - \frac{1}{2}\right] + \frac{C_A}{2}\ln\left(\frac{t_1}{u_1}\right) \tag{4}$$

where $C_F = (N_c^2 - 1)/(2N_c)$ and $C_A = N_c$, with $N_c = 3$ the number of colors. Two-loop [14, 15] and three-loop [17] expressions are also available but they are not required for the NLL accuracy that we use here.

The aNLO soft-gluon corrections for $gq \to tA$ are

$$\frac{d^2\hat{\sigma}_{gq \to tA}^{(1)}}{dt\,du} = F_{gq \to tA}^{\text{LO}}\frac{\alpha_s(\mu_R^2)}{\pi}\left\{c_3\left[\frac{\ln(s_4/m_t^2)}{s_4}\right]_+ + c_2\left[\frac{1}{s_4}\right]_+ + c_1\delta(s_4)\right\}\,, \tag{5}$$

where $c_3 = 2(C_F + C_A)$,

$$c_2 = 2C_F\ln\left(\frac{u_1}{t_2}\right) - C_F + C_A\ln\left(\frac{t_1}{u_1}\right) + C_A\ln\left(\frac{sm_t^2}{u_2^2}\right) - (C_F + C_A)\ln\left(\frac{\mu_F^2}{m_t^2}\right)\,, \tag{6}$$

$$c_1 = \left[C_F\ln\left(\frac{-t_2}{m_t^2}\right) + C_A\ln\left(\frac{-u_2}{m_t^2}\right) - \frac{3}{4}C_F\right]\ln\left(\frac{\mu_F^2}{m_t^2}\right) - \frac{\beta_0}{4}\ln\left(\frac{\mu_F^2}{\mu_R^2}\right)\,, \tag{7}$$

μ_F is the factorization scale, μ_R is the renormalization scale, and $\beta_0 = (11C_A - 2n_f)/3$ is the lowest-order QCD β function, with $n_f = 5$ the number of light-quark flavors.

The aNNLO soft-gluon corrections for $gq \to tA$ are

$$
\begin{aligned}
\frac{d^2\hat{\sigma}_{gq \to tA}^{(2)}}{dt\,du} &= F_{gq \to tA}^{\text{LO}}\frac{\alpha_s^2(\mu_R^2)}{\pi^2}\left\{\frac{1}{2}c_3^2\left[\frac{\ln^3(s_4/m_t^2)}{s_4}\right]_+ + \left[\frac{3}{2}c_3 c_2 - \frac{\beta_0}{4}c_3\right]\left[\frac{\ln^2(s_4/m_t^2)}{s_4}\right]_+ \right. \\
&\quad + \left[c_3 c_1 - (C_F + C_A)^2\ln^2\left(\frac{\mu_F^2}{m_t^2}\right) - 2(C_F + C_A)c_2\ln\left(\frac{\mu_F^2}{m_t^2}\right) + \frac{\beta_0}{4}c_3\ln\left(\frac{\mu_R^2}{m_t^2}\right)\right]\left[\frac{\ln(s_4/m_t^2)}{s_4}\right]_+ \\
&\quad \left. + (C_F + C_A)\left[-c_1\ln\left(\frac{\mu_F^2}{m_t^2}\right) - \frac{\beta_0}{4}\ln\left(\frac{\mu_F^2}{m_t^2}\right)\ln\left(\frac{\mu_R^2}{m_t^2}\right) + \frac{\beta_0}{8}\ln^2\left(\frac{\mu_F^2}{m_t^2}\right)\right]\left[\frac{1}{s_4}\right]_+\right\}\,. \tag{8}
\end{aligned}
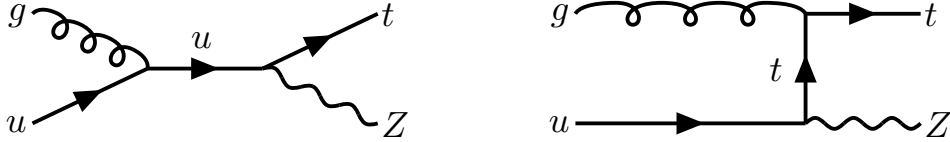$$

3 $gu \to tZ$ via anomalous top-quark couplings

Figure 1: Tree-level diagrams for tZ production via anomalous couplings.

We first present results for $gu \to tZ$ production. The LO Feynman diagrams contributing to the process are shown in Fig. 1. Numerical results for the total cross section are given in Fig. 2. We use MMHT2014 [18] NNLO parton distribution functions (PDFs) and take $\kappa_{tqZ} = 0.01$. The results in [14] use CT14 [19] PDFs; however, those results are very similar to the ones presented here. The left plot shows the total aNNLO cross section as a function of top quark mass at LHC energies of 7, 8, 13, and 14 TeV, with K-factors relative to aNLO shown in the inset. We show a more detailed breakdown at 13 TeV LHC energy in the right plot, showing LO, aNLO, aNNLO, and aNNNLO cross sections, as well as K-factors over LO in the inset. We find that the increase in the cross section is substantial at aNNLO for all energies in the plots, with a 49% increase in the total cross section at 13 TeV at aNNLO compared to the 36% increase at aNLO. The further contribution from aNNNLO corrections is much smaller.
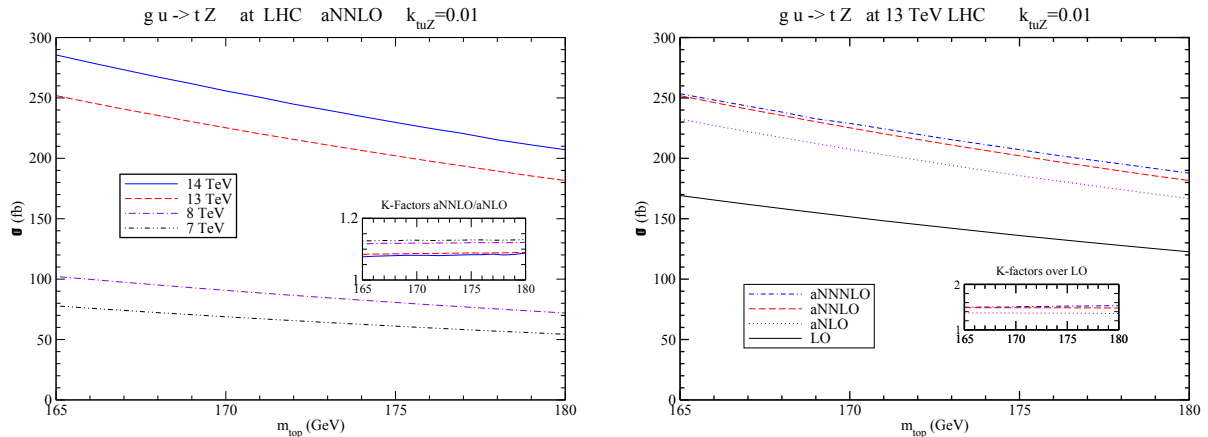

Figure 2: The left plot shows results for the total aNNLO cross section for $gu \to tZ$ at 7, 8, 13, and 14 TeV as a function of top-quark mass. Its inset shows aNNLO/aNLO K-factors. The right plot shows the total LO, aNLO, aNNLO, and aNNNLO cross section at 13 TeV as a function of top-quark mass. Its inset shows K-factors relative to LO.

Differential distributions in top-quark rapidity and transverse momentum are shown in Fig. 3, where we see a similarly significant impact by the higher-order corrections. For more details on the soft-gluon corrections to $gq \to tZ$ and further numerical results, including results for charm-quark initial states and scale dependence, see Ref. [14].

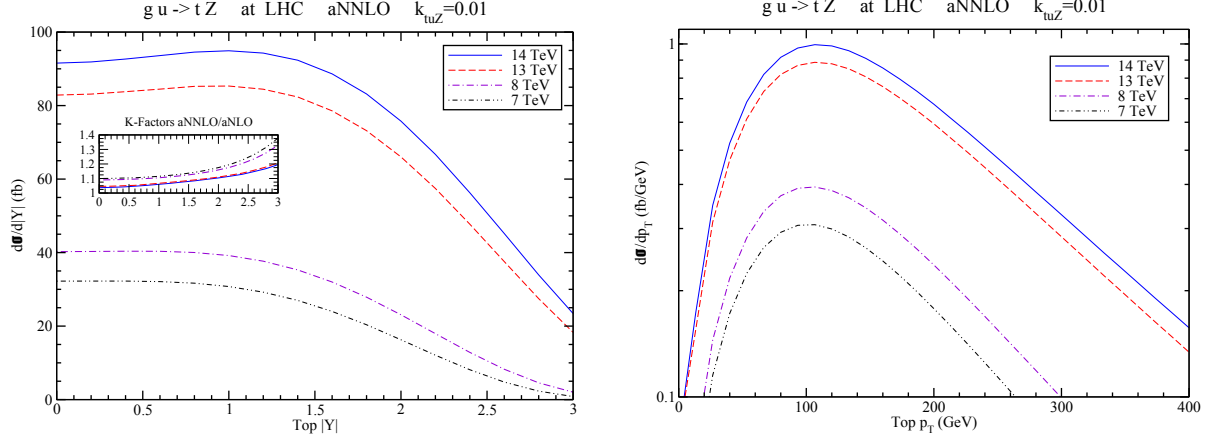Figure 3: Differential aNNLO rapidity (left plot) and transverse-momentum (right plot) distributions for $gu \to tZ$ at LHC energies of 7, 8, 13, and 14 TeV. The inset of the rapidity plot also includes K-factors over aNLO.

4 $gu \to t\gamma$ via anomalous top-quark couplings

Figure 4: Tree-level diagrams for $t\gamma$ production via anomalous couplings.

We continue with results for $gu \to t\gamma$. The LO Feynman diagrams describing the process are shown in Fig. 4, and are analogous to those for $gu \to tZ$. Just as with the process $gu \to tZ$, we use MMHT2014 [18] NNLO PDFs and take $\kappa_{tq\gamma} = 0.01$. The left plot shows results for the total aNNLO cross section as a function of top-quark mass at LHC energies of 7, 8, 13, and 14 TeV, with K-factors relative to aNLO shown in the inset. The right plot shows a more detailed breakdown at 13 TeV of the total cross section at LO, aNLO, aNNLO, and aNNNLO, with K-factors over LO shown in the inset. Similarly to $gu \to tZ$, we find a significant increase in the cross section at aNLO and aNNLO, with much smaller contributions from aNNNLO. At 13 TeV, the NLO corrections provide a 31% increase in the cross section, and the aNNLO results provide a 36% increase. The differential distributions shown in Fig. 6 experience a similarly significant increase by the higher-order corrections. For more details on the soft-gluon corrections to $gq \to t\gamma$ and further numerical results, including scale dependence and results for charm-quark initial states, see Ref. [15].
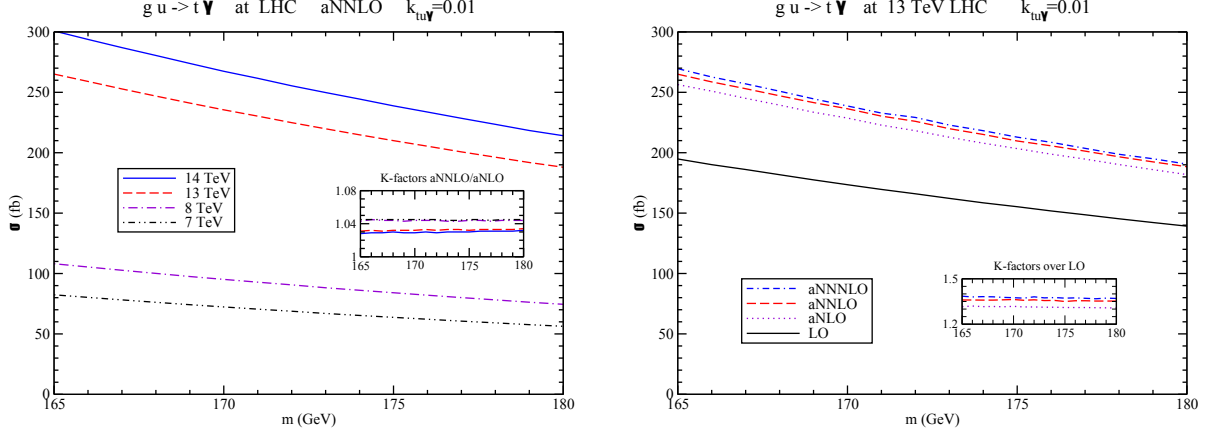
Figure 5: The left plot shows results for the total aNNLO cross section for $gu \to t\gamma$ at 7, 8, 13, and 14 TeV as a function of top-quark mass. Its inset shows aNNLO/aNLO K-factors. The right plot shows the total LO, aNLO, aNNLO, and aNNNLO cross section at 13 TeV as a function of top-quark mass. Its inset shows K-factors relative to LO.
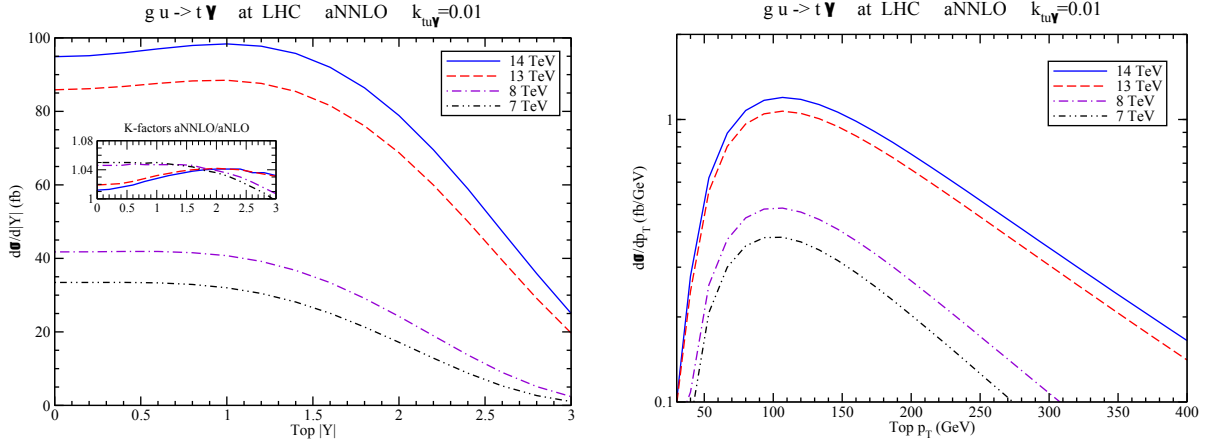

Figure 6: Differential aNNLO rapidity (left plot) and transverse-momentum (right plot) distributions for $gu \to t\gamma$ at LHC energies of 7, 8, 13, and 14 TeV. The inset of the rapidity plot also includes K-factors over aNLO.

5 Conclusions

In some physics models beyond the Standard Model, it is possible to have tZ and $t\gamma$ production without any additional quarks in the final state. In order to have better experimental limits on these anomalous couplings, we have studied higher-order corrections to both the total cross sections and differential distributions for $gq \to tZ$ and $gq \to t\gamma$. These corrections dominate the cross section numerically, and approximate well [14,15] the complete corrections at NLO [6,12]. At aNNLO, they contribute up to a 36% increase at 13 TeV for $gu \to t\gamma$ and 49% increase at 13 TeV for $gu \to tZ$. Future work will study soft-gluon corrections in processes with more than two particles in the final state.

Acknowledgements

References

[1] CMS Collaboration, JHEP 04 (2016) 035 [`arXiv:1511.03951`]

[2] CMS Collaboration, JHEP 07 (2017) 003 [`arXiv:1702.01404`]

[3] ATLAS Collaboration, ATLAS-CONF-2017-070.

[4] T. Tait and C.-P. Yuan, Phys. Rev. D **63**, 014018 (2000) [hep-ph/0007298].

[5] N. Kidonakis and A. Belyaev, JHEP **12**, 004 (2003) [hep-ph/0310299].

[6] Y. Zhang, B.H. Li, C.S. Li, J. Gao, and H.X. Zhu, Phys. Rev. D **83**, 094003 (2011) [arXiv:1101.5346].

[7] M. Fael and T. Gehrmann, Phys. Rev. D **88**, 033003 (2013) [arXiv:1307.1349].

[8] J. Adelman *et al.*, arXiv:1309.1947.

[9] C. Degrande, F. Maltoni, J. Wang, and C. Zhang, Phys. Rev. D **91**, 034024 (2015) [arXiv:1412.5594].

[10] G. Durieux, F. Maltoni, and C. Zhang, Phys. Rev. D **91**, 074017 (2015) [arXiv:1412.7166].

[11] Y.-C. Guo, C.-X. Yue, and S. Yang, Eur. Phys. J. C **76**, 596 (2016) [arXiv:1603.00604].

[12] B.H. Li, Y. Zhang, C.S. Li, J. Gao, and H.X. Zhu, Phys. Rev. D **83**, 114049 (2011) [arXiv:1103.5122].

[13] J.-L. Agram, J. Andrea, E. Conte, B. Fuks, D. Gele, and P. Lansonneur, Phys. Lett. B **725**, 123 (2013) [arXiv:1304.5551].

[14] N. Kidonakis, Phys. Rev. D **97**, 034028 (2018) [`arXiv:1712.01144`]

[15] M. Forslund and N. Kidonakis, Phys. Rev. D **98**, 074017 (2018) [`arXiv:1808.09014`].

[16] N. Kidonakis, Int. J. Mod. Phys. A **33**, 1830021 (2018) [arXiv:1806.03336].

[17] N. Kidonakis, Phys. Rev. D **99**, 074024 (2019) [arXiv:1901.09928].

[18] L.A. Harland-Lang, A.D. Martin, P. Molytinski, and R.S. Thorne, Eur. Phys. J. C **75**, 204 (2015) [`arXiv:1412.3989`].

[19] S. Dulat, T.-J. Hou, J. Gao, M. Guzzi, J. Huston, P. Nadolsky, J. Pumplin, C. Schmidt, D. Stump, and C.-P. Yuan, Phys. Rev. D **93**, 033006 (2016) [`arXiv:1506.07443`].